International Journal on Advanced Science Engineering Information Technology

Vol.12 (2022) No. 2
ISSN: 2088-5334

Mechanical Properties of the Stereolithography Resin with Different Printing Configurations.

Fernanda Boada [a], Cosme Mejia-Echeverria [a,*], David Ojeda [a]

[a] *Mechatronic Department-GISIBI research group, Universidad Técnica del Norte, Av. 17 de Julio 5-2, Ibarra, 100105, Ecuador*
Corresponding author: [*]cdmejia@utn.edu.ec

***Abstract*— In the 3D printer market, there are several types of printing; among those found in the middle are fused filament deposition printing and stereolithography. In stereolithography, layers of resin are solidified employing UV rays. Each manufacturer offers different types of resins that react to light exposure. These usually have very general values in terms of their mechanical strength, with varying properties depending on the printing configurations. For this reason, the user, in many cases, must make trial and error prints to obtain the best possible printing configuration, generating expenses and waste of material. This research proposes establishing the appropriate printing parameters to obtain the best mechanical properties of the prototypes printed in the digital light process stereolithography printer of the Universidad Tecnica del Norte. A specimen fabrication process based on the ASTM D638 standard is established, in which the main printing configurations are varied, such as printing orientation, layer thickness, and light exposure time. Experimental tensile tests obtain deformation stress-strain curves. From this, the behavior of the printed material is obtained as linear elastic-fragile. The results obtained are compared concerning the maximum stress and strain, and the modulus of elasticity is calculated. The most suitable printing parameters are proposed to obtain the best results in stereolithography printing for the construction of functional prototypes.**

***Keywords*— Stereolithography; mechanical properties; 3D printing; resin; materials.**

Manuscript received 21 May. 2021; revised 16 Sep. 2021; accepted 24 Nov. 2021. Date of publication 30 Apr. 2022.

I. INTRODUCTION

Within the stages of creating a product, prototyping is a crucial facet. The designer can obtain different concrete answers from the design. Analyzing if the manufacturing methods and the materials are being used in the different components of the product are the right ones. Because the prototype is manufactured with different manufacturing methods than the mass-produced product, it is necessary that the prototype has good fidelity to the final product [1]–[4].

Within the manufacture of plastic components, the prototype can be made employing 3D printing, but at the time of mass production, the most feasible option is the method of plastic injection into molds. For this reason, an appropriate distribution within the design is required between the fidelity, time, effort, and cost required for the manufacture of the prototype. In the industry, we handle prototypes that can be built quickly and economically but still have a great fidelity to provide the designer with the information that is being sought [5]–[9]. The objective of prototyping is to identify the weakest points at an early stage of the design to increase the quality of the final product. For this reason, it is important to have a component with mechanical characteristics similar to those of the final product, which allows finding more precisely the part most susceptible to mechanical failure. In addition, reducing the amount of material used in parts with an excessive safety factor and saving costs in mass production by offering a reliable and good quality product [1], [10]–[12].

The manufacturing processes based on additive manufacturing tend to elaborate on mechanical elements because of the speed of the elaboration of a physical prototype to measure. It is important to analyze the printing parameters by stereolithography to contribute to the development of prototypes [13]–[16].

A printed object can have different mechanical properties in 3D printing by Fused Deposition Modeling (FDM). This is because FDM printers melt plastic layers onto already melted and solidified layers, creating a mechanical (not chemical) bond. Therefore, the printed parts will be anisotropic, depending on how the mechanical stress is applied. The direction with the highest mechanical performance is the direction in which the material is deposited. It comprises the direction with the lowest mechanical performance is the same

as the axis in which the filaments and layers of the printing are joined. The bonding between the layers causes permeabilities in the final product due to the presence of microscopic holes [17]–[20].

In stereolithography 3D printing (SLA), unlike FDM, the layers are held together without microscopic holes due to the chemical covalent bonds between them when the resin solidifies in each layer. This increases the forces that hold the layers together, improving the mechanical strength properties in the direction of the axis in which the layers are constructed. These chemical bonds are generated at each layer cure by a reaction that generates the polymerization of the resin of both the previous layer and the new layer. The covalent bonds are generated in all directions, and when evaluating the difference between the xy-plane and the z-plane, it is minimal. In this type of printing, the products are impermeable and completely dense [17], [21], [22].

SLA was developed by Dr. Hideo Kodama in 1981 and became the oldest additive manufacturing (AM) technology, considered as a fast and economical method to reconstruct products in space (3 Dimensions). This technology was generated in advance of the holographic technique [23].

SLA was initially used for modeling and prototyping applications. However, several studies analyzed this technique in constructing complex geometries in which the technique was very efficient. In addition, the possibility of extending the range of materials to include metals and ceramics was observed. At the moment, all the analyses and studies of this technique specify that the process is designed to be done on only one material at a time, with the difference that a better surface finish can be obtained [23]–[25].

SLA is a polymerization method in which resin (liquid precursor) is placed in a tank to be exposed to ultraviolet (UV) light, which causes its solidification at the points of incidence of the same. The polymeric reaction starts when the resin's Photo Initiator (PI) molecules receive irradiation in the specific zone. With the solidified layer, a new layer is generated in which resin enters and will be irradiated and cured. Performing this process layer by layer, a prototype is built [23], [26]–[28].

Depending on the direction of the incident light, SLA can be applied in two different ways; from the top, known as free surface focusing, or from the bottom of a transparent tank in restricted surface focusing [10], [23].

The SLA technology has several forms of execution: the first is the SLA-laser, in which a laser is in charge of irradiating the points of the corresponding layer section; the second is digital light processing (DLP), in which an image projects the layer to be solidified onto the resin tank, influencing it at the same time in all the points of the layer to be solidified. There is another method, little used, in which a liquid crystal display (LCD) is used, through a mask, to present the layer to be solidified [3], [10], [29].

DLP is a method that achieves resolutions between 0.6µm and 25 µm. Under this same process, it has been possible to introduce ceramic particles [23], [30], [31]. DLP is excellent for illuminating sharp corners but can cause surface roughness [32].

At the Universidad Técnica del Norte, a project was developed to develop a 3D stereolithography printer for the simulation and CNC machining laboratory; it allows the development of prototypes for different branches of biomechanical research, manufacturing processes, material sciences, etc. [33]. Table 1 shows the main characteristics of the printer to be used in this research.

TABLE I
UTN-DLP PRINTER FEATURES [33].

Printing method	**SLA-DLP**
SVGA Resolution	2800 lumens
Printing area (mm)	200 * 200 * 400

The resins for stereolithography are a type of polymer that, when exposed to ultraviolet light, changes its physical and mechanical properties, forming a physical differentiation between the exposed and unexposed parts. In this case, the photoresin only solidifies in the area that receives the light while the area that does not receive it remains in a liquid state [34]–[36].

In today's market, there are many kinds of photoresists, some of which are elastic, rigid, flexible, high-temperature resident, among others [37], in which the following research can be applied to provide more fidelity to the final prototype and give the designer closer information to the final product[38], [39].

In the present study, three types of resins are analyzed (Table 2). According to their properties, the most suitable one is selected for the development of the project. Among the most important factors when selecting the resin is to ensure that it is suitable for printing on DLP, with a wavelength of 405 nm for curing, unlike the resin used for SLA-laser that uses a wavelength of 385 nm [23].

TABLE II
BRANDS OF RESIN MANUFACTURERS FOR STEREOLITHOGRAPHY RELEVANT IN THE MARKET[27]–[29].

Resin Brands	**Tensile Strength (MPa)**	**Strain (%)**	**Wavelength (nm)**
Hard Join 3D ®	15	4	Not specified
AnyCubic ®	23,4	14,2	405
Kudo 3D ®	34,9	1,2	400-440

The Hard Join 3D resin is ideal for creating objects without compression capacity under forces, presents some contraction, being this of rapid cure. The objects cannot be bent or expanded and are characterized by high tensile properties, shear, and low elongation [27].

Advantages of high solidification, the speed with strong adhesion of the model, ease to disassemble after formation, rigid are important parameters that Anycubic offers being this a stable material under different climatic conditions, in addition, it is easy to store, overcoming the deficiencies of other resins that are easily wetted and environmental corrosion [29].

A high resolution and a smooth surface are the characteristics of Kudo 3D resin (3DSR UHR) manufacturers. Prints with this resin are identified with professional equipment. It is widely used in the research area.[28]. After reviewing the current state of research and the use of technology, we proceed to propose a methodology for analyzing the object of study.

II. Materials and Method

A. Standard Specimens

The clear AnyCubic® resin is selected to manufacture the specimens according to type V of the ASTM D638-14 standard. This standard is applicable for determining the tensile properties of reinforced and unreinforced plastics. "The test method is applicable for testing materials of any thickness up to 14 mm (0.55 in.)"[30].

The dimensions to be applied for the design of the specimen are shown in Table 3

TABLE III
V-Type Specimen Dimensions [30]

Dimensions	Value (mm)	Tolerance
W-Narrow section width	3.18	±0.5
L-Narrow section length	9.53	±0.5
WO-Total width	9.53	3.18
LO-Total length	63.5	…
G-Calibrated length	7.62	±0.25

This type of specimen specifies that it will be used when a limited material with a thickness of up to 4mm (0.16 in.), this model is used when a large number of specimens are required, and the material for their manufacture is scarce or expensive. The suggested number of specimens to be made is five for stress testing of isotropic materials and suggests that specimens with defects be discarded. A test speed of 1, 10, or 100 mm/min for type V specimen should be used[30].

B. Manufacture of the Specimens

Three different settings are selected to print the specimens, as shown in Figure 1, to proceed to print them on the UTN-DLP printer.

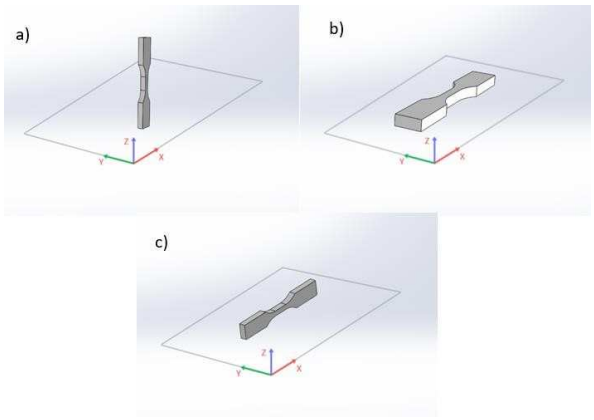

Fig. 1 Orientation: a) vertical, b) horizontal c) lateral

It is used as a base for the impression the adhesive tape Abro® P.O. 1174, which has a smooth surface and as an advantage the material (resin) is not absorbed, avoiding in a certain way the waste of the material and on it the Scotch ® tape 233+ which allows the detachment of the piece without fractures.

The different configurations used in the printer and the printing of the necessary specimens to develop the traction analysis are detailed. In these configurations, the curing time and thickness per layer, printing characteristics identified as relevant and influencing the mechanical properties of the printed part, are modified.

1) Configuration of the horizontal specimens: In this arrangement, the direction of the tensile load coincides with the direction of the impression layer. On the other hand, three types of configurations were made in this group. The variables to be modified are the curing time and the thickness per layer. The curing time was maintained in the three configurations for the present case, as shown in Table 4. The thickness per layer is the variable analyzed to establish its effect on the mechanical properties of the test specimens.

TABLE IV
Curing times and thickness per layer configurations horizontal printing

Curing time (s)	**Conf. 1**	**Conf. 2**	**Conf. 3**
Adhesion Layer	27	27	27
Normal Layer	6	6	6
Layer thickness(µm)	**Conf. 1**	**Conf. 2**	**Conf. 3**
Adhesion Layer	50	100	150
Normal Layer	100	150	200

2) Configuration of the lateral specimens: In this arrangement, the direction of the tensile load coincides with the direction of the impression layer. In this case, the thickness per layer was maintained in all three configurations. As can be seen in table 5, the curing time is modified to analyze the effect it can have on the mechanical properties of the test specimens.

TABLE V
Curing time and thickness per layer configuration side printing

Curing time (s)	**Conf. 1**	**Conf. 2**	**Conf. 3**
Adhesion Layer	27	30	35
Normal Layer	6	10	15
Layer thickness(µm)	**Conf. 1**	**Conf. 2**	**Conf. 3**
Adhesion Layer	50	50	50
Normal Layer	100	100	100

3) Configuration of the vertical specimens: In this arrangement, the direction of the tensile load is perpendicular to the direction of the impression layer. An analysis of the influence of print orientation on the mechanical properties of the specimens is desired. Therefore, the direction of orientation was vertical while maintaining a fixed layer thickness and a variation in the curing time, as shown in table 6.

TABLE VI
Curing time and thickness per layer configutrations vertical printing

Curing time (s)	**Conf. 1**	**Conf. 2**	**Conf. 3**
Adhesion Layer	27	30	35
Normal Layer	6	10	15
Layer thickness(µm)	**Conf. 1**	**Conf. 2**	**Conf. 3**
Adhesion Layer	50	50	50
Normal Layer	100	100	100

For each type of orientation, there are three different specimen configurations in which the parameters of thickness per layer and curing time change; a total of 45 specimens are printed and subjected to destructive (tensile) testing.

C. Testing Machine

A Universal James Heal Titan 10 testing machine located in the mechanical testing laboratory of the Universidad Técnica del Norte is used to carry out the mechanical tensile

tests. The test is performed at 100 mm/min with an ambient temperature of 25º C and relative humidity of 50%.

Specimens that had fractures outside the test zone (Figure 2) were removed as test specimens and replaced.

Fig. 2 Discarded Specimens

III. Results and Discussion

A. Results of the Mechanical Tensile Test

After the tests have been carried out, the strain-strain curves are obtained, which in all cases show the behavior of the linear fragile elastic material. We proceed to obtain the maximum stress and average strain values for each type of specimen. From these data, the average modulus of elasticity is calculated, taking into account the linear behavior of the material. The average results can be seen in table 7

TABLE VII
AVERAGE RESULTS OF TENSILE TESTS

Conf.	Ultimate tensile Stress (Mpa)	Strain (mm/mm)	Elasticity Module (MPa)
Group 1 "Horizontal orientation			
1	18.095	0.13866	130.49
2	16.055	0.13313	120.60
3	21.748	0.12050	180.49
Group 2 "Lateral Orientation			
1	27.155	0.20684	131.28
2	30.036	0.15279	196.58
3	40.552	0.16922	239.64
Group 3 " Vertical Orientation			
1	28.445	0.20276	140.29
2	41.178	0.16088	255.97
3	38.417	0.15916	241.38

B. Analysis of Mechanical Properties vs Printing Parameters

The tensile strength of the lateral and vertical orientation is almost twice the strength of the horizontal orientation. Therefore, the direction of loading must be taken into account when printing parts.

1) Maximum stress with a variation of curing time: Figure 3 shows the prints in the three-position settings with a fixed print layer of 100 µm for each, with a variation of curing time of 6, 10, and 15 seconds.

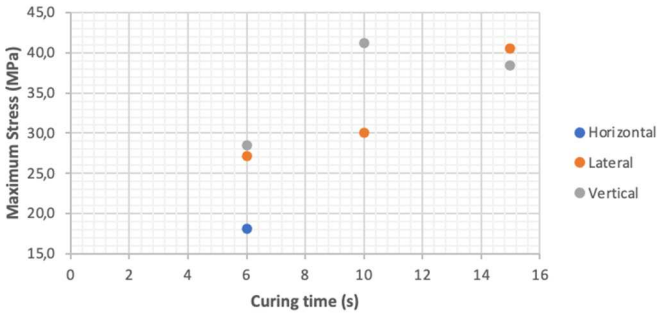

Fig. 3 Maximum stress with a variation of curing time

When analyzing at 6 s and 10s, the vertical configuration has greater mechanical resistance than the others; it is observed that from 10s it tends to stabilize at the value of its maximum stress being the best configuration for when the curing time varies.

2) Maximum stress with a variation of layer thickness: Figure 4 shows three different layer thickness configurations with a constant cure time of 6 seconds.

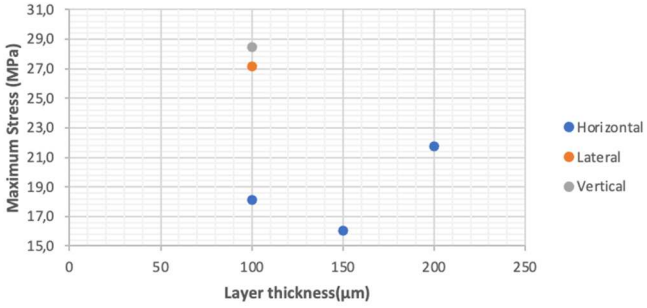

Fig. 4 Maximum stress with a variety of layer thickness

When analyzing the horizontal orientation, it is shown that the specimen with a layer thickness of 100 µm increases its stress considerably by doubling the thickness to 200 µm. The maximum stress is obtained from the vertical configuration exceeds the stress of the horizontal configuration by 56.44%.

3) Maximum strain with a variation of curing time: The specimens that show the most strain have the shortest curing time, as shown in figure 5; the horizontal orientation achieves the least strain.

By increasing the curing time to 10 and 15 seconds, the vertically oriented specimens come to stabilize their strain value.

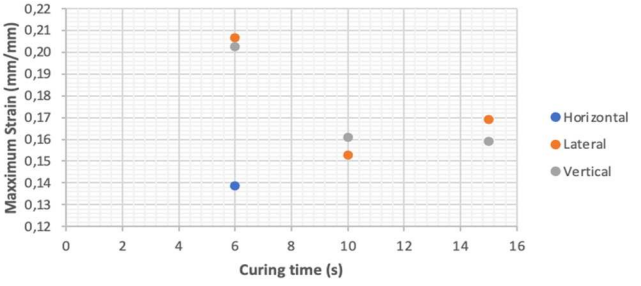

Fig. 5 Maximum strain with a variation of curing time

4) Maximum strain with Layer Thickness variation: Figure 6 shows the strain graph as a function of the layer

thickness. Increasing the thickness per layer with horizontal orientation results in less strain.

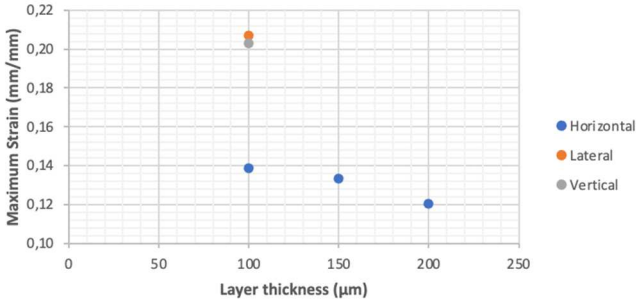

Fig. 6 Maximum strain with a variation of layer thickness

With a layer thickness of 100 µm, a greater deformation is obtained with a lateral orientation similar to the vertical one, leaving the horizontal orientation well below.

5) Comparison with a modulus of elasticity: Figure 7 and figure 8 show that the material becomes more rigid at all position settings when the print time is increased, or the print layer is doubled.

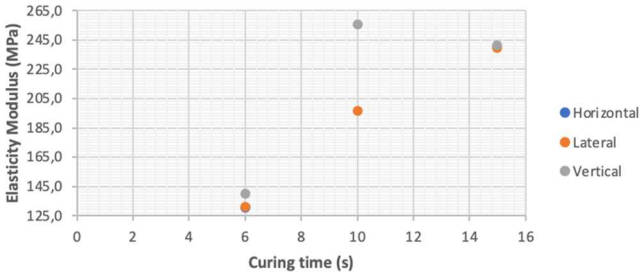

Fig. 7 Modulus of elasticity with variation in curing time

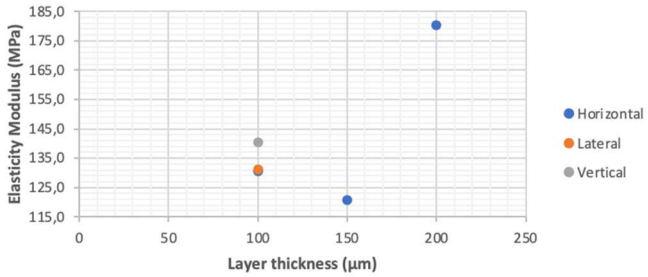

Fig. 8 Modulus of elasticity with variation in layer thickness

C. Proposal of printing parameters

Once the results of each configuration have been compared, we recommend the appropriate parameters in stereolithography printing using transparent 405 nm resin. The printing must be executed with layers perpendicular to the direction to which the force is going to be applied, a configuration that showed the best values in mechanical resistance since the object is totally immersed in the resin and the surface of the layer is cured simultaneously.

This printing orientation presents the best mechanical properties in the tensile test since it obtains ultimate tensile stress values of up to an additional 60% provided by the resin manufacturers. The adequate layer thickness in this type of printing with which a good mechanical resistance and deformation are achieved by using layers of multiples of 100 µm. The minimum cure time for good performance is at least 10 s per 100 µm of a layer.

IV. Conclusion

Layer thicknesses between 100 µm and 200 µm with variations of 50 µm were established for the horizontal, vertical, and lateral print configurations with curing times of 6, 10 and 15 seconds; for the manufacture of type V specimens according to ASTM 638. Prints with a higher mechanical resistance than those provided by the resin manufacturer are obtained from curing times higher than 10s per layer, evidencing that the lower times suggested by the manufacturer do not generate a fine print or exceed the indicated mechanical resistance. It is evident that prints with a 60% improvement in mechanical resistance are obtained with thicknesses of at least 100 µm; concerning the values provided by the resin manufacturer. The prints show an increase of rigidity proportional to the increase of the layer thickness and the curing time due to higher exposure to the resin radiation. The experiment results show that a print with better mechanical properties is obtained when the print layer is perpendicular to the direction in which the force is to be exerted, confirming the polymer chemical bond between DLP-SLA print layers.

The direction of the printing layer influences the tensile strength of the material. It was found that if the load applied to a specimen coincides with the direction of the printing layer, and its contact surface per layer is higher; its resistance will be approximately half concerning loads whose direction is perpendicular to that of the printing layer; or which have the same direction but with a smaller contact surface.

References

[1] S. and D. D. and G. R. and D. L. and A. J. and Y. A. and J. A. and S. D. and K. C. and I. P. Cantrell Jason and Rohde, "Experimental Characterization of the Mechanical Properties of 3D Printed ABS and Polycarbonate Parts," in *Advancement of Optical Methods in Experimental Mechanics, Volume 3*, 2017, pp. 89–105, doi: https://doi.org/10.1007/978-3-319-41600-7_11.

[2] B. K. Suryatal, S. S. Sarawade, and S. P. Deshmukh, "Fabrication of medium scale 3D components using stereolithography system for rapid prototyping," *Journal of King Saud University - Engineering Sciences*, 2021, doi: https://doi.org/10.1016/j.jksues.2021.02.012.

[3] J. Borrello, P. Nasser, J. C. Iatridis, and K. D. Costa, "3D printing a mechanically-tunable acrylate resin on a commercial DLP-SLA printer," *Additive Manufacturing*, vol. 23, pp. 374–380, 2018, doi: https://doi.org/10.1016/j.addma.2018.08.019.

[4] B. T. Phillips *et al.*, "Additive manufacturing aboard a moving vessel at sea using passively stabilized stereolithography (SLA) 3D printing," *Additive Manufacturing*, vol. 31, p. 100969, 2020, doi: https://doi.org/10.1016/j.addma.2019.100969.

[5] C. D. Hernández Castellano *et al.*, *Tecnologías de Fabricación Aditiva*. Universidad de Las Palmas de Gran canaria, 2018.

[6] A. Shrotri, M. Beyer, D. Schneider, and O. Stübbe, "Manufacturing of lens array prototypes containing spherical and fresnel lenses for visible light communications using stereolithography apparatus," in *Laser 3D Manufacturing VIII*, Mar. 2021, doi: 10.1117/12.2586907.

[7] K. and P. E. and K. S. and S. N. and V. J. Madheswaran S. and Sivakumar, "Applications of Additive Manufacturing—A Review," in *Advances in Materials Research*, 2021, pp. 21–27, doi: https://doi.org/10.1007/978-981-15-8319-3_3.

[8] JM. Jafferson and S. Pattanashetti, "Use of 3D printing in production of personal protective equipment (PPE) - a review," *Materials Today: Proceedings*, Feb. 2021, doi: 10.1016/j.matpr.2021.02.072.

[9] V. Lemarteleur *et al.*, "3D-printed protected face shields for health care workers in Covid-19 pandemic," *American Journal of Infection*

Control, vol. 49, no. 3, pp. 389–391, 2021, doi: https://doi.org/10.1016/j.ajic.2020.08.005.
[10] S. Waheed *et al.*, "3D printed microfluidic devices: enablers and barriers," *Lab Chip*, vol. 16, no. 11, pp. 1993–2013, 2016, doi: 10.1039/C6LC00284F.
[11] I. Chan, J. Au, C. Ho, and J. Lam, "Creation of 3D printed fashion prototype with multi-coloured texture: a practice-based approach," *International Journal of Fashion Design, Technology and Education*, vol. 14, no. 1, pp. 78–90, 2021, doi: 10.1080/17543266.2020.1861342.
[12] C. Varghese, J. Wolodko, L. Chen, M. Doschak, P. P. Srivastav, and M. S. Roopesh, "Influence of Selected Product and Process Parameters on Microstructure, Rheological, and Textural Properties of 3D Printed Cookies," *Foods*, vol. 9, no. 7, 2020, doi: 10.3390/foods9070907.
[13] A. Quezada and A. Rigail, "Evaluacion De Polietilenos De Alta Densidad Reciclados Para Aplicaciones En Mobiliario Urbano," 2007.
[14] R. E. Rebong, K. T. Stewart, A. Utreja, and A. A. Ghoneima, "Accuracy of three-dimensional dental resin models created by fused deposition modeling, stereolithography, and Polyjet prototype technologies: A comparative study," *The Angle Orthodontist*, vol. 88, no. 3, pp. 363–369, Mar. 2018, doi: 10.2319/071117-460.1.
[15] D. T. Pham, S. S. Dimov, and R. S. Gault, "Part Orientation in Stereolithography," *The International Journal of Advanced Manufacturing Technology*, vol. 15, no. 9, pp. 674–682, 1999, doi: 10.1007/s001700050118.
[16] M. Manoj Prabhakar, A. K. Saravanan, A. Haiter Lenin, I. Jerin leno, K. Mayandi, and P. Sethu Ramalingam, "A short review on 3D printing methods, process parameters and materials," *Materials Today: Proceedings*, vol. 45, pp. 6108–6114, 2021, doi: https://doi.org/10.1016/j.matpr.2020.10.225.
[17] G. Garrido Sánchez, "Diseño y fabricación de un dedo protésico articulado mediante impresión 3D," 2019.
[18] T.-C. Yang and C.-H. Yeh, "Morphology and Mechanical Properties of 3D Printed Wood Fiber/Polylactic Acid Composite Parts Using Fused Deposition Modeling (FDM): The Effects of Printing Speed," *Polymers*, vol. 12, no. 6, 2020, doi: 10.3390/polym12061334.
[19] M. Kamaal, M. Anas, H. Rastogi, N. Bhardwaj, and A. Rahaman, "Effect of FDM process parameters on mechanical properties of 3D-printed carbon fibre–PLA composite," *Progress in Additive Manufacturing*, vol. 6, no. 1, pp. 63–69, 2021, doi: 10.1007/s40964-020-00145-3.
[20] S. Wickramasinghe, T. Do, and P. Tran, "FDM-Based 3D Printing of Polymer and Associated Composite: A Review on Mechanical Properties, Defects and Treatments," *Polymers*, vol. 12, no. 7, 2020, doi: 10.3390/polym12071529.
[21] B. Msallem, N. Sharma, S. Cao, F. S. Halbeisen, H.-F. Zeilhofer, and F. M. Thieringer, "Evaluation of the Dimensional Accuracy of 3D-Printed Anatomical Mandibular Models Using FFF, SLA, SLS, MJ, and BJ Printing Technology," *Journal of Clinical Medicine*, vol. 9, no. 3, 2020, doi: 10.3390/jcm9030817.
[22] A. Katheng, M. Kanazawa, M. Iwaki, and S. Minakuchi, "Evaluation of dimensional accuracy and degree of polymerization of stereolithography photopolymer resin under different postpolymerization conditions: An in vitro study," *The Journal of Prosthetic Dentistry*, vol. 125, no. 4, pp. 695–702, 2021, doi: https://doi.org/10.1016/j.prosdent.2020.02.023.
[23] C. Schmidleithner, "Stereolithography," in *3D Printing*, D. M. K. E.-D. Cvetković, Ed. Rijeka: IntechOpen, 2018, p. Ch. 1.
[24] Z. Tian, Y. Yang, Y. Wang, H. Wu, W. Liu, and S. Wu, "Fabrication and properties of a high porosity h-BN–SiO2 ceramics fabricated by stereolithography-based 3D printing," *Materials Letters*, vol. 236, pp. 144–147, 2019, doi: https://doi.org/10.1016/j.matlet.2018.10.058.
[25] A. Bagheri Saed, A. H. Behravesh, S. Hasannia, S. A. Alavinasab Ardebili, B. Akhoundi, and M. Pourghayoumi, "Functionalized poly l-lactic acid synthesis and optimization of process parameters for 3D printing of porous scaffolds via digital light processing (DLP) method," *Journal of Manufacturing Processes*, vol. 56, pp. 550–561, 2020, doi: https://doi.org/10.1016/j.jmapro.2020.04.076.
[26] H. Song, N. A. Rodriguez, C. C. Seepersad, R. H. Crawford, M. Chen, and E. B. Duoss, "Development of a variable tensioning system to reduce separation force in large scale stereolithography," *Additive Manufacturing*, vol. 38, p. 101816, 2021, doi: https://doi.org/10.1016/j.addma.2020.101816.
[27] Y. Sano, R. Matsuzaki, M. Ueda, A. Todoroki, and Y. Hirano, "3D printing of discontinuous and continuous fibre composites using stereolithography," *Additive Manufacturing*, vol. 24, pp. 521–527, 2018, doi: https://doi.org/10.1016/j.addma.2018.10.033.
[28] I. Valizadeh, A. al Aboud, E. Dörsam, and O. Weeger, "Tailoring of functionally graded hyperelastic materials via grayscale mask stereolithography 3D printing," *Additive Manufacturing*, vol. 47, p. 102108, 2021, doi: https://doi.org/10.1016/j.addma.2021.102108.
[29] R. He *et al.*, "Fabrication of complex-shaped zirconia ceramic parts via a DLP- stereolithography-based 3D printing method," *Ceramics International*, vol. 44, no. 3, pp. 3412–3416, 2018, doi: https://doi.org/10.1016/j.ceramint.2017.11.135.
[30] A. della Bona, V. Cantelli, V. T. Britto, K. F. Collares, and J. W. Stansbury, "3D printing restorative materials using a stereolithographic technique: a systematic review," *Dental Materials*, vol. 37, no. 2, pp. 336–350, 2021, doi: https://doi.org/10.1016/j.dental.2020.11.030.
[31] H. Quan, T. Zhang, H. Xu, S. Luo, J. Nie, and X. Zhu, "Photo-curing 3D printing technique and its challenges," *Bioactive Materials*, vol. 5, no. 1, pp. 110–115, 2020, doi: https://doi.org/10.1016/j.bioactmat.2019.12.003.
[32] D. A. Komissarenko *et al.*, "DLP 3D printing of scandia-stabilized zirconia ceramics," *Journal of the European Ceramic Society*, vol. 41, no. 1, pp. 684–690, 2021, doi: https://doi.org/10.1016/j.jeurceramsoc.2020.09.010.
[33] P. A. Heredia López and C. D. Mejía Echeverría, "Impresora 3D por estereolitografía," Universidad Técnica del Norte, 2018.
[34] F. Cosmi and A. Dal Maso, "A mechanical characterization of SLA 3D-printed specimens for low-budget applications," *Materials Today: Proceedings*, vol. 32, pp. 194–201, 2020, doi: https://doi.org/10.1016/j.matpr.2020.04.602.
[35] H. Xing, B. Zou, S. Li, and X. Fu, "Study on surface quality, precision and mechanical properties of 3D printed ZrO2 ceramic components by laser scanning stereolithography," *Ceramics International*, vol. 43, no. 18, pp. 16340–16347, 2017, doi: https://doi.org/10.1016/j.ceramint.2017.09.007.
[36] X. Y. Yap *et al.*, "Mechanical properties and failure behaviour of architected alumina microlattices fabricated by stereolithography 3D printing," *International Journal of Mechanical Sciences*, vol. 196, p. 106285, 2021, doi: https://doi.org/10.1016/j.ijmecsci.2021.106285.
[37] I. Gil, "La impresión 3D y sus alcances en la arquitectura," 2015.
[38] R. Pandey, "Photopolymers in 3D printing applications," 2014.
[39] E. D. V. Niño, J. L. Endrino, H. A. E. Durán, A. Díaz-Lantada, B. Pérez-Gutiérrez, and A. D. Lantada, "Caracterización microscópica de texturas superficiales fabricadas aditivamente mediante estereolitografía láser = Microscopy characterization of superficial textures additively manufactured by laser stereolithography = Caracterizaão microscópica de texturas superficiais fabricadas aditiva por estereolitografia laser," *Respuestas*, vol. 21, no. 2, pp. 37–47, Jul. 2016, [Online]. Available: http://oa.upm.es/55415/.
[40] Photocentrics, "Ficha Técnica BR3D-DL-CASTABLE Resinas Calcinables polímeros 3D," 2016. [Online]. Available: www.photocentricgroup.com.
[41] Kudo3D Inc, "3DSR UHR Resin," 2019. Accessed: May 08, 2021. [Online]. Available: https://www.kudo3d.com/resin-2/#3dsr-uhr.
[42] Formlabs INC, "Materials Data Sheet Photopolymer Resin for Form 1+ and Form 2," 2019.
[43] ASTM International, "ASTM D638-14, Standard Test Method for Tensile Properties of Plastics," West Conshohocken, PA, 2014. doi: 10.1520/D0638-14.